ChemComm

Accepted Manuscript

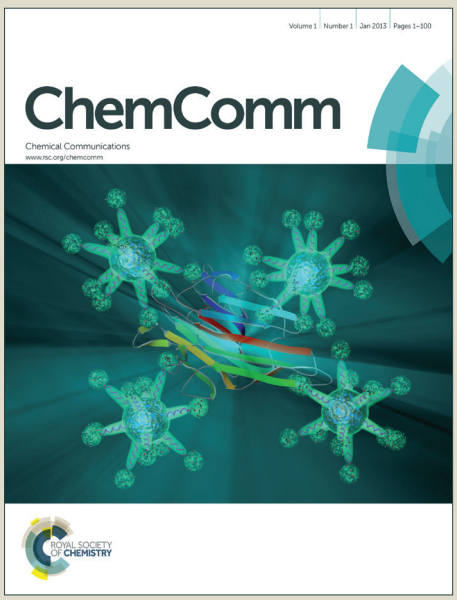

ROYAL SOCIETY OF CHEMISTRY

www.rsc.org/chemcomm

Journal Name

RSCPublishing

COMMUNICATION

$^{15}N_2$ formation and fast oxygen isotope exchange during pulsed $^{15}N^{18}O$ exposure of MnO_x/CeO_2

Cite this: DOI: 10.1039/xoxxoooooox

J. Szanyi[a*] and J.H. Kwak[a,b]

Received ooth January 2012,
Accepted ooth January 2012

DOI: 10.1039/xoxxoooooox

www.rsc.org/

Pulsing $^{15}N^{18}O$ onto an annealed 1% $Mn^{16}O_x/Ce^{16}O_2$ catalyst resulted in very fast oxygen isotope exchange and $^{15}N_2$ formation at 295 K. In the 1st $^{15}N^{18}O$ pulse, due to the presence of large number of surface oxygen defects, extensive $^{15}N_2{}^{18}O$ and $^{15}N_2$ formations were observed. In subsequent pulses oxygen isotope exchange dominated as a result of highly labile oxygen in the oxide.

The oxidation of NO to NO_2 is a key reaction in catalytic soot oxidation, since NO_2 is a more efficient oxidant than molecular O_2.[1-3] Precious metal-based catalysts have been shown to be effective in this reaction, however, it is important to minimize the use of these metals in large volume catalytic processes due to their limited availability.[4-6] To this end there have been attempts to develop cheaper, oxide-based catalysts for the oxidation of NO to NO_2 at the relatively low temperatures Diesel engines operate at.[7-12] CeO_2 has long been used as an additive in automotive exhaust treatment catalysis due to its oxygen storage capacity.[13-15] Recently MnO_x-doped CeO_2 was reported to exhibit high NO oxidation activity.[16] The key feature of an efficient oxidation catalyst should be its high propensity to provide activated oxygen (oxygen atoms) to the reactant, in this case to NO. This requires high mobility of oxygen in these oxide systems. The addition of metal oxide to CeO_2 has been shown to enhance its oxygen mobility, and therefore, its reactivity, for example in ethanol steam reforming.[17]

NO interacts strongly with both CeO_2 and MnO_x/CeO_2 forming a series of surface NO_x species (hyponitrites, nitrites, nitrates).[18-20] Exposing these reducible oxides to NO has been shown to result in the formation of N_2O even at ambient temperatures.[20] The key reaction intermediate proposed in this reaction was a surface hyponitrite species $(N_2O_2)^{2-}$ formed in two adjacent oxygen vacancy sites on the ceria surface. When a large excess of O_2 is present in the reactant gas mixture containing NO competition for the vacancy sites on the surface of reducible oxide will take place between O_2 and NO. The mobility of oxygen species on the ceria surface (at low temperature) and in the bulk (at high temperature) is critical to achieve high oxidation efficiency.

In this communication we provide evidence for the formation of $^{15}N_2$ over a 1% MnO_x/CeO_2 catalyst upon its interaction with $^{15}N^{18}O$ at 295 K. Furthermore, we will show that very fast oxygen isotope exchange takes place between the oxide and the adsorbed NO_x species, confirming the high mobility of oxygen on/in this metal oxide catalyst. (MnO_x-free CeO_2 shows very similar behaviour to the 1% MnO_x/CeO_2 discussed here (Fig. S1), while pure MnO_2 displays much slower rate of oxygen isotope exchange (Fig. S2) and produces no N_2 or N_2O.)

All the experiments were carried out in a system that consists of an FTIR spectrometer, IR cell, mass spectrometer and gas delivery system. The catalysts studied were pre-treated prior to $^{15}N^{18}O$ exposure in situ by annealing at 773 K in vacuum, and in some cases by oxidation or reduction at 773 K. The catalysts then were exposed to $^{15}N^{18}O$ pulses and the changes in the gas composition (MS) and the surface species formed (FTIR) were followed as a function of time (the cell was evacuated after each pulse). After the completion of each pulse experiment (3-5 pulses) the IR cell was evacuated and a temperature programmed desorption was carried out.

The gas phase composition as a function of time-on-stream recorded from an annealed 1% MnO_x/CeO_2 sample at 295 K is displayed in Fig. 1.

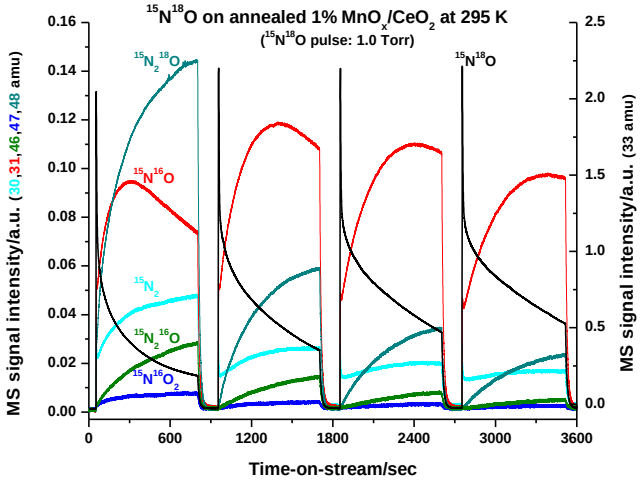

Figure 1. Variation of gas phase composition during pulsed $^{15}N^{18}O$ exposure of an annealed 1% MnO_x/CeO_2 catalyst at 295 K. ($^{15}N_2$: 30 amu; $^{15}N^{16}O$: 31 amu; $^{15}N^{18}O$: 33 amu; $^{15}N_2{}^{16}O$: 46 amu; $^{15}N^{16}O_2$: 47 amu; $^{15}N_2{}^{18}O$: 48 amu)

Upon the introduction of the first $^{15}N^{18}O$ aliquot several new ^{15}N-containing species appear in the gas phase: $^{15}N_2$, $^{15}N^{16}O$, $^{15}N_2{}^{16}O$, $^{15}N_2{}^{18}O$, $^{15}N^{16}O_2$. At the same time the intensity of the 33 amu signal ($^{15}N^{18}O$) decreases very fast as a result of two main processes that take place in the system: adsorption of $^{15}N^{18}O$ on the catalyst surface, and conversion of some of the adsorbed species to ^{15}N-containing compounds listed above. The highest initial rate of formation is observed for $^{15}N^{16}O$ (red trace in Fig. 1), the product of isotopic exchange between ^{16}O of the ceria lattice and ^{18}O in the incoming $^{15}N^{18}O$ pulse. With time on stream the partial pressure of $^{15}N^{16}O$ reaches a maximum and then drops. In contrast, the MS signal of $^{15}N_2{}^{18}O$ increases throughout the duration of the 1st $^{15}N^{18}O$ pulse, and becomes the dominant species in the gas phase at t>300 sec. The very fast $^{15}N^{16}O$ formation results in the appearance of increasing amount of $^{15}N_2{}^{16}O$, which probably forms as a result of re-adsorption of the initially produced $^{15}N^{16}O$ molecules. Interestingly, a significant amount of $^{15}N_2$ is also detected, and the profile of the 30 amu MS signal closely follows those of both $^{15}N_2{}^{18}O$ (48 amu) and $^{15}N_2{}^{16}O$ (46 amu). This observation suggests that the formation of molecular nitrogen is related to the nitrous oxide. (One may argue that the entire 30 amu MS signal originate from the cracking of nitrous oxide in the ionization chamber of the mass spectrometer. However, when we introduced N_2O into the mass spectrometer the ratio of the 28 and 44 amu signals was much lower than what we observed during the NO pulsing experiments. Nevertheless, it is evident that part of the 30 amu MS signal originates from the cracking of the N_2O in the MS.) It is also interesting to note that during the first $^{15}N^{18}O$ pulse the formation of $^{15}N^{16}O_2$ (47 amu) is clearly evident, but under no conditions we have observed the formation of either $^{15}N^{16}O^{18}O$ (49 amu) or $^{15}N^{18}O_2$ (51 amu) (see Fig. S3) due, most probably, to the very fast isotope exchange between the adsorbed NOx molecules and the surface.

In order to understand the processes taking place during the interaction of $^{15}N^{18}O$ with the 1% MnO_x/CeO_2 sample, IR spectra were collected during the first $^{15}N^{18}O$ pulse (Fig. 2). The IR features observed can be assigned to NO^-, $(N_2O_2)^{2-}$ and NO_2^- surface species. The assignments were based on the results of prior studies of NO_x adsorption on CeO_2 and MnO_x/CeO_2 materials.[19-22] The most intense peak at 1141 cm^{-1} (together with the 796 and 1241 cm^{-1} ones) represents chelating NO_2^- species, while broader feature centered at 1082 cm^{-1} has contributions from both cis- and trans-$(N_2O_2)^{2-}$ (ν_{asym}(N-O)). The ν_{asym}(N-N) vibrations of these two species are observed at 1314 (cis) and 1380 cm^{-1} (trans). The 1773 cm^{-1} feature is associated with the ν_{asym}(N-O) vibration of adsorbed cis-$(NO)_2$, while the band at around 2167 cm^{-1} originate from the ν_{asym}(N-N) vibration of adsorbed N_2O molecules. No nitrate formation was observed in any pulsed experiments conducted at 295 K.

NO as an amphoteric molecule can interact by two fundamentally different ways with the oxide surface:[20] (a) transferring one electron to the surface and interacting with both the thus formed Ce^{3+} and lattice O^{2-} ions to produce the chelating NO_2^- species and (b) accepting one electron from a surface defect site (Ce^{3+}) to form NO^- and $(N_2O_2)^{2-}$ species. Since the 1% MnO_x/CeO_2 sample was annealed at 773 K prior to exposure to the first pulse of $^{15}N^{18}O$, a large number of surface defects were created under these reducing conditions (evidenced by the O_2^- (1125 cm^{-1}) and O_2^{2-} (835 cm^{-1}) species formed on the annealed CeO_2 sample upon O_2 exposure at 295 K (Fig. S4)). The removal of every lattice O^{2-} ion creates two Ce^{3+} defect sites, providing adsorption sites for the incoming NO molecules. On these associated defect sites the formation of NO-dimers (hyponitrite ions) is facile, as the IR spectra reveal the fast formation of these species. Concomitant to the development of IR features representing these adsorbed surface species is the appearance of an IR band at 2167 cm^{-1} of adsorbed $^{15}N_2{}^{18}O$. The formation of N_2O on ceria surfaces has been reported previously and was associated with the decomposition of adsorbed $(N_2O_2)^{2-}$ species. The facile decomposition of hyponitrites on this catalyst at 295 K is evidenced by the fast increase in the partial pressure of $^{15}N_2{}^{18}O$. The formation of $^{15}N_2$ can be attributed to either the direct decomposition of $(N_2O_2)^{2-}$ to $^{15}N_2$ and $^{18}O_2{}^{2-}$ or to the decomposition reaction of the initially formed $^{15}N_2{}^{18}O$ on the catalysts to $^{15}N_2$ and ^{18}O. We prefer the consecutive reaction path for $^{15}N_2$ formation, since the probability of breaking two N-O bonds simultaneously in the adsorbed $(^{15}N_2{}^{18}O_2)^{2-}$ species should be very low.

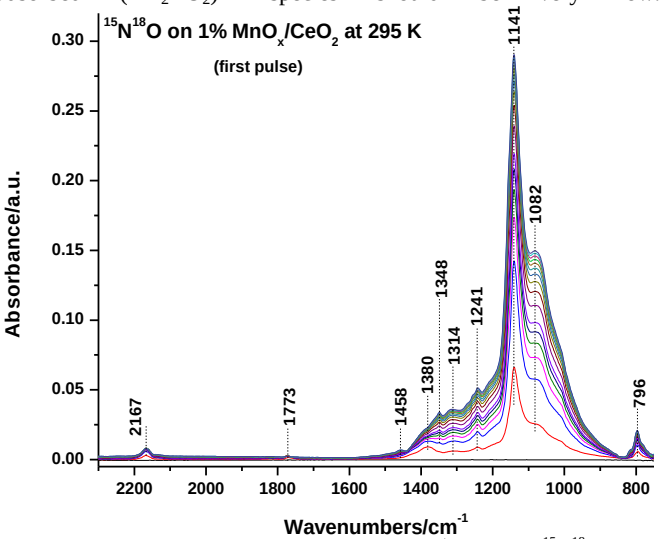

Figure 2. FTIR spectra collected during the 1st pulse of $^{15}N^{18}O$ of an annealed 1% MnO_x/CeO_2 catalyst at 295 K.

Very pronounced changes in gas phase composition can be seen in subsequent $^{15}N^{18}O$ pulses: the prominent species in pulses 2-5 is $^{15}N^{16}O$. At the same time, the concentration of $^{15}N_2{}^{18}O$ decreases dramatically in the 2nd pulse and continuously decreases in subsequent pulses. Most of the changes observed in the gas phase after the 1st $^{15}N^{18}O$ pulse can be explained by the changes in the catalyst surface upon its interaction with $^{15}N^{18}O$. Most importantly, the number of oxygen vacancies decreases dramatically as $^{15}N_2{}^{18}O$ and $^{15}N_2{}^{16}O$ are formed. Therefore, the most important process taking place on the catalyst surface is the isotope exchange between ^{18}O in the adsorbed $^{15}N^{18}O$ molecules and the ^{16}O atoms of the ceria lattice. This process is very facile even in subsequent $^{15}N^{18}O$ pulses (large amount of $^{15}N^{16}O$ is produced even in the 5th $^{15}N^{18}O$ pulse). With increasing number of $^{15}N^{18}O$ pulse the overall conversion of $^{15}N^{18}O$ decreases, as it is evidenced by the increasingly higher partial pressure of $^{15}N^{18}O$ in the IR cell at the completion of each pulse (~900 sec). This is due, mostly, to the gradual enrichment of the ceria surface layer with ^{18}O. However, this process is still very fast even in the 5th $^{15}N^{18}O$ pulse.

After the completion of the 5th $^{15}N^{18}O$ pulse the adsorbed surface species were removed from the sample by temperature programmed desorption (TPD) (from 295 to 773 K at 12 K/min heating rate, in vacuum). The MS intensities of selected mass fragments and a series of IR spectra collected during TPD are displayed in panels *a* and *b* of Fig. 3, respectively. Below 400 K the primary desorbing species is weakly held $^{15}N^{18}O$ (33 amu) and $^{15}N^{16}O$ (31 amu), the first one with higher intensity. A small amount of $^{15}N_2{}^{18}O$ (48 amu) is also seen to evolve from the catalyst at this low temperature. The maximum desorption rate of the major desorption product ($^{15}N^{16}O$) is observed at around 520 and 680 K, and originate from desorption of strongly adsorbed surface species. The intensity of the 31 amu fragment ($^{15}N^{16}O$) is about seven times higher in the first high temperature desorption peak (~520 K) than that of the 33 amu

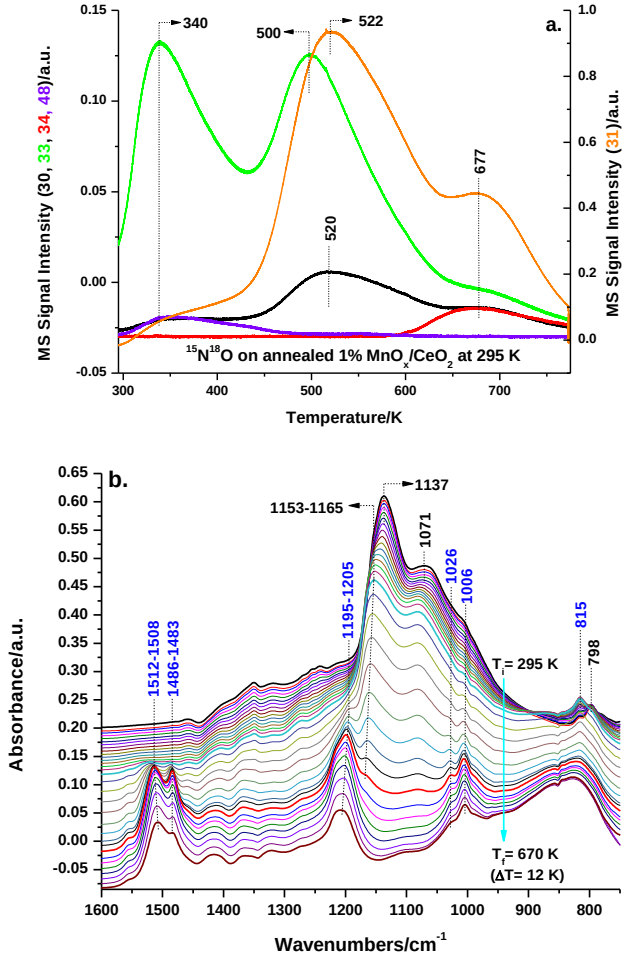

Figure 3. Selected MS (a) traces and FTIR (b) spectra recorded during TPD following five pulses of $^{15}N^{18}O$ on an annealed 1% MnO_x/CeO_2 catalyst at 295 K. (heating rate=12 K/min)

($^{15}N^{18}O$) one. Due to the very fast oxygen isotope exchange between ^{18}O atoms present in the strongly adsorbed surface species ($^{15}N^{18}O_x^-$ and $(^{15}N^{18}O_2)^{2-}$) and the lattice ^{16}O atoms during the TPD process. This isotope scrambling results in blueshifts of the IR features centered at 1137 and 798 cm^{-1} (initially formed $^{15}N^{16}O^{18}O^-$) to 1153 and 815 cm^{-1} ($^{15}N^{16}O_2^-$) as the sample is heated from 295 to ~475 K. In this temperature range only the weakly held, molecularly adsorbed species (mostly $^{15}N^{18}O$ and $^{15}N_2{}^{18}O$) desorb while all the ionic NO_x species stay on the surface. Between 450 and 600 K the IR features of nitrites and hyponitrites gradually decreases, and concomitantly, a very intense $^{15}N^{16}O$ TPD feature develops (peak temperature at ~520 K). At the same time we can also observe the evolution $^{15}N_2$ into the gas stream. These observations can be explained by the thermal decomposition of nitrite and hyponitrite species in this temperature range. Two main processes seem to take place in parallel: decomposition (to give the large 31 amu signal) of nitrites/hyponitrites and conversion of nitrites to nitrates. This latter process is evidenced by the appearance and intensification of IR bands characteristic of nitrate species (1450-1550 cm^{-1} and 980-1050 cm^{-1}). The extra oxygen atom required to convert nitrites to nitrates can come from two sources in this system: from the oxide bulk, and from the decomposition of hyponitrites. Our data cannot distinguish between these two nitrate formation processes, but it is possible that in a parallel process as nitrites convert to nitrates the oxygen vacancies created in the oxide are filled by oxygen atoms from the decomposition of hyponitrites. Above 600 K nitrates decompose mostly as $^{15}N^{16}O$ and $^{16}O_2$ (not shown) with the evolution of a small amount of $^{16}O^{18}O$ (34 amu). Only traces of $^{18}O_2$ evolution were observed during nitrate decomposition. Furthermore, the intensity of the $^{15}N^{18}O$ signal (33 amu) is very low in this temperature range. All these observations suggest that most of the ionic NO_x species (nitrites and nitrates) contain mostly ^{16}O atoms as a result of extensive oxygen isotope exchange with the oxide catalyst.

Conclusions

Oxygen vacancies on an annealed 1% MnO_x/CeO_2 catalyst are responsible for the facile formation of both $^{15}N_2{}^{18}O$ and $^{15}N_2$ upon its exposure to $^{15}N^{18}O$ even at 295 K. The extensive isotope exchange between $^{15}N^{18}O$ and the oxide catalyst underlines the high mobility of lattice oxygens in the mixed-oxide catalyst that may contribute to its enhanced NO oxidation activity.

We gratefully acknowledge the US Department of Energy (DOE), Office of Energy Efficiency and Renewable Energy/Vehicle Technologies Program for the support of this work. The research described in this paper was performed at the Environmental Molecular Sciences Laboratory (EMSL), a national scientific user facility sponsored by the DOE's Office of Biological and Environmental Research and located at Pacific Northwest National Laboratory (PNNL). PNNL is operated for the US DOE by Battelle.

Notes and references

[a] Institute for Integrated Catalysis, Pacific Northwest National Laboratory, Richland, WA 99352, USA
[b] Current Address: Department of Chemical Engineering, UNIST, Ulsan, S. Korea

1. R. Allanson, B.J. Cooper, J.E. Thoss, A. Uusimaki, A.P. Walker, J.P. Warren, *SAE* 2000 Paper No. 2000-01-0480 .
2. K. Yoshida, S. Makino, S. Sumiya, G. Muramatsu, R. Helferich, *SAE* 1989 Paper No. 892046 .
3. B.J. Cooper, J.E. Thoss, *SAE* 1989 Paper No. 890404 .
4. R. Matarrese, L. Castoldi, L. Lietti, P. Forzatti, *Top. Catal*. 2007, **42**, 293.
5. A. Setiabudi, M. Makkee, J.A. Moulijn, *Top. Catal*. 2004, **30**, 305.
6. R.S. Zhu, M.X. Guo, F. Ouyang, *Catal. Today* 2008, **139**, 146.
7. Y. Teraoka, K. Kanada, S. Kagawa, *Appl. Catal. B: Environmental* 2001, **34**, 73.
8. R. Lopez-Fonseca, U. Elizundia, I. Landa, M.A. Gutierrez-Ortiz, J.R. Gonzalez-Velasco, *Appl. Catal. B: Environmental* 2005, **61**, 150.
9. X.D. Wu, Q. Liang, D. Weng, Z.X. Lu, *Catal. Commun*. 2007, **8**, 2110.
10. F.E. Lopez-Suarez, A. Bueno- Lo pez, M.J. Illan-Go mez, A. Adamski, B. Ura, J.Trawczynski, *Environ. Sci. Technol*. 2008, **42**, 7670.
11. F.E. Lo pez-Sua rez, S. Parres-Esclapez, A. Bueno-Lopez, M.J. Illan-Go mez, B. Ura, J.Trawczynski, *Appl. Catal. B: Environmental* 2009, **93**, 82.
12. I. Atribak, A. Bueno-Lo pez, A. Garcıa-Garcıa, P. Navarro, D. Frıas, M. Montes, *Appl.Catal. B: Environmental* 2010, **93,** 267.
13. A. Bueno-Lo pez, K. Krishna, M. Makkee, J.A. Moulijn, *J. Catal*. 2005, **230**, 237.
14. E. Aneggi, C. de Leitenburg, G. Dolcetti, A. Trovarelli, *Catal. Today* 2006, **114**, 40.
15. A. Setiabudi, J. Chen, G. Mul, M. Makkee, J.A. Moulijn, *Appl. Catal. B: Environmental* 2004, **51**, 9.
16. W. Wang, G. McCool, N. Kapur, G. Yuan, B. Shan, M. Nguyen, U.M. Graham, B.H. Davis, G. Jacobs, K. Cho, X. Hao, *Science*, 2012, **337**, 832-835.
17. H. Song, U.S. Ozkan, *J.Phys.Chem. A*, 2010, **114**, 3796-3801.
18. J. Soria, A. Martinez-Arias, J.C. Conesa, *J.Chem.Soc. Faraday Trans.*, 1995, **91**, 1669-1678.
19. A. Martinez-Arias, J. Soria, J.C. Conesa, X.L. Seoane, A. Arcoya, R, Cataluna, , *J.Chem.Soc. Faraday Trans.*, 1995, **91**, 1679-1687.
20. G. Qi, R.T. Yang, R. Chang, *Appl. Catal. B: Environmental*, 2004, **51**, 93-106.
21. B. Azambre, L. Zenboury, F. Delacroix, J.V. Weber, *Catal. Today*, 2008, **137**, 278-282.
22. L. Goldbloom, M.H. Hughes, B.C. Stace, *Spectrochim.Acta*, 1976, **32A**, 1345-1346.